engineering proceedings

MDPI

Proceeding Paper

Direct Description of Inherent Strains for Thin-Plate Welding Distortion Modelling †

Asle J. Tomstad *, Ivan Bunaziv and Magnus Eriksson

Materials and Nanotechnology, SINTEF Industry, NO-7465 Trondheim, Norway; ivan.bunaziv@sintef.no (I.B.); magnus.eriksson@sintef.no (M.E.)

* Correspondence: asle.joachim.tomstad@sintef.no

† Presented at the 16th International Aluminium Conference (INALCO 2026), Trondheim, Norway, 10–12 June 2026.

Abstract

Numerically efficient and user-friendly modelling of component distortions is the key for enabling numerical design of thin-plate structures accounting for welding distortions. This especially concerns large structures, e.g., bridges or ship panels. The direct description of inherent strains is a method for introducing inherent strains into a commercial finite element solver. The presented version utilizes thermo-mechanical local modelling with 3D solid elements in Abaqus as a source for the inherent distortion fields. The resulting inherent strain fields are post-processed and subsequently applied to a low-fidelity component model utilizing 3D thin shell elements in Abaqus. The new direct description method of introducing the inherent strain fields for thin shell elements is presented in this paper, and it shows promising results.

Keywords: welding distortions; finite element simulations; inherent strain method; thin-plate structures; thin shell elements

1. Introduction

Welding deformations readily occur in welded thin-plate structures, and they are a critical factor influencing production/construction, acceptance criterion for weld defects and structural performance. Accurate, computationally efficient, and user-friendly methods for modelling of component distortions is one key element for enabling numerical design of thin-plate structures accounting for welding distortions. The concept of inherent strains bulks and quantifies the in-elastic strains, which are considered to cause distortions [1,2]. The inherent strains method allows for applying the result of a thermo-mechanical process without the need to model the entire thermo-mechanical history. In turn, the inherent strain method allows for computationally efficient simulations of complex structures, and it is extensively used in residual stress analysis and distortion analysis. Large structures comprising multiple welds, especially thin-plate structures, provide a numerical challenge, as the thickness of the plates constrains either the size of the idealized model or the resolution of the model, i.e., limiting the element size. Marine structures such as ships have motivated previous research on this topic, prompting techniques for introducing inherent strain into computationally efficient 3D-shell element meshes, e.g., refs. [3–5] implemented the layered approach into an in-house finite element solver. Another example is Qweld [6,7]. Commercial code implementations include the implementation of the layered approach [8–10] or strain as a direct boundary method [11]. The novel approach

Check for updates

Academic Editor: Sigmund Arntsønn Tronvoll

Published: 18 August 2026

Copyright: © 2026 by the authors. Licensee MDPI, Basel, Switzerland. This article is an open access article distributed under the terms and conditions of the Creative Commons Attribution (CC BY) license.

proposed in the present work for describing the three-dimensional distortion field using 3D shell elements is based on the well-known inherent strain theory, with a direct description of both the uniform and through thickness variations in the in-plane normal inherent strains. The main focus of this paper is the implementation and demonstration of an efficient method for introducing inherent strains into 3D shell element models. The method is implemented in the commercial finite element code Abaqus via a UEXPAN subroutine to impose the inherent strain field on the 3D shell elements. High-fidelity thermo-mechanical local modelling using 3D solid elements in Abaqus is employed as the source of the inherent distortion fields. The resulting inherent strain fields are post processed and subsequently applied to a low-fidelity component model utilizing 3D thin shell elements in Abaqus. The new implementation for describing inherent strain fields in thin shell elements shows promising results and is validated against experimental distortion measurements from a two-pass thin-plate fillet T joint.

2. Materials and Methods

2.1. Experimental

The experimental work consists of four specimens comprising a 70 mm wide × 150 mm long and 5 mm thick extruded 6082 aluminum plate, denoted P1, welded to the middle of a 150 mm wide × 150 mm long and 5 mm thick extruded 6082 aluminum plate, herein denoted P2. The geometry is visualized in Figure 1, wherein the weld is highlighted as the red section. The plates were welded together by GMAW (Gas Metal Arc Welding) by a two-pass fillet and using a 5183 welding wire. The welding parameters used were the following: a wire feed rate of 8.6 m/min, a current of 154 A, and a voltage of 18.4 V. The plates were left to cool for 600 s between the two passes.

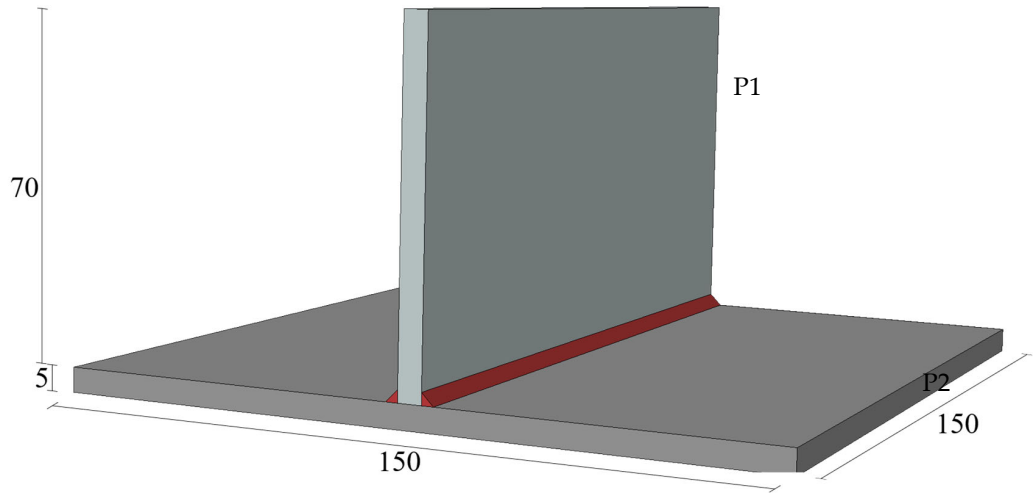


Figure 1. The nominal specimen geometry, showing the fillet weld in red.

2.2. Numerical

2.2.1. Themo-Mechanical "High-Fidelity" Model

The numerical work consists of two parts; the first part is a "high-fidelity" finite element simulation which is used as a source for inherent strains that are post-processed and subsequently applied to the second part, i.e., the "low-fidelity" 3D-shell finite element model. A brief description of the "high-fidelity" model is provided; however, the focus is on the "low-fidelity" model and it will therefore remain the primary focus of this paper.

The "high-fidelity" model consists of 3D solid finite elements in an uncoupled-thermo-mechanical model. The finite element mesh is shown in Figure 2, and the mesh is refined towards the welded zone. The "high-fidelity" thermo-mechanical modelling framework is

not fully optimized, and due to this several simplifications were used: The base material (light grey) and the weld material (green) are provided with the same thermo-mechanical parameters. For the heat transfer simulation, the materials were given the density of 2.7×10^{-3} g/mm^3, the thermal conductivity of 0.120 W/mmK and the specific heat of 0.9 J/gK. For the mechanical simulation, the materials were given a constant thermal expansion coefficient of 2.66×10^{-5} 1/K, and a thermo-elastic–plastic material model was applied. The content of the J_2-dependent thermo-elastic–plastic material model is, at the time of writing, unpublished work, and will be disseminated at a later date. Time-dependent progressive element activation was used in both the heat transfer simulation and the thermo-mechanical simulation, and the rate of activation corresponded to the (room temperature) volume of filler wire added per second. The heat source was modelled as the commonly employed Gaussian volumetric heat source via DFLUX subroutine [12].

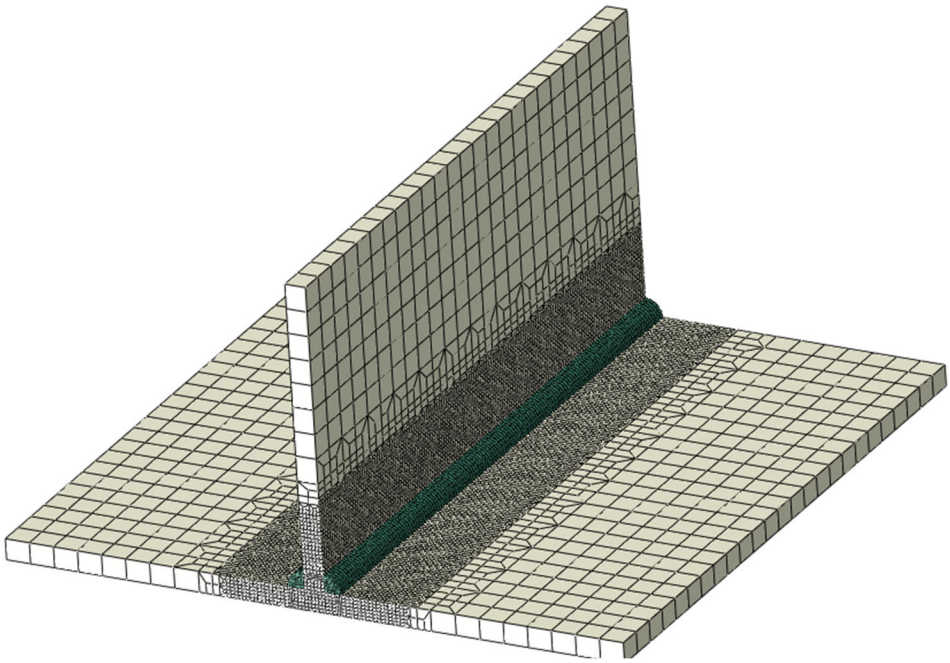


Figure 2. 3D solid finite element mesh, whereas the fillet mesh is colored green.

2.2.2. Direct Description of Inherent Strains

The direct description of inherent strains is a method of implementing the venerable inherent strain method into a commercial finite element solver. Similar to the layered approach, this method assumes that the distortion field (longitudinal shrinkage, transverse shrinkage, longitudinal bending and transverse bending) may be modelled with the in-plane strains. Figures 3 and 4 depict the application of in-plane normal strains; whereas, Figure 3 depicts the direct description method, and Figure 4 depicts the layered approach.

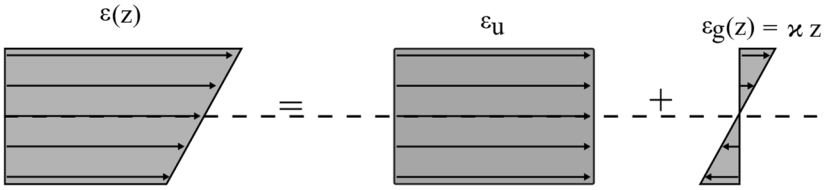


Figure 3. Application of through-thickness strain gradient using the direct description.

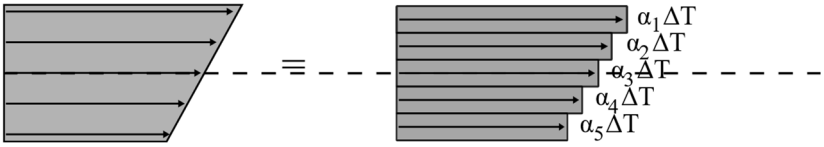


Figure 4. Application of through-thickness strain gradient using the layered approach, shown here for 5 layers.

In both figures, the strain field is shown to the left, while the discretization of the strain field with the respective method is shown to the right of the equal sign. In the case of direct description method, the strain field is discretized as a uniform part, ε_u, and a part representing the gradient ε_g. The former part contributes to the shrinkage while the latter contributes to the out of plane bending. Here the gradient is assumed to vary linearly with respect to the curvature $\varkappa$. In the case of the layered approach, the strain field is discretized as stacked layers; whereas, the magnitude (strain) is determined by the strain value sampled at the middle of the layer. A common way of applying the layered strains is to utilize "composite lay-up" with individual thermal expansion coefficients.

One benefit of the layered approach is that there is no need for any implementation of subroutines; however, it is significantly more cumbersome to apply the inherent strains as each layer for each considered element must be described with unique thermal expansion coefficients. However, bulking the behaviour of elements would reduce the number of assigned coefficients.

In Abaqus, the direct description method requires the implementation of a user subroutine, and the simplest method is to utilize a UEXPAN, and an incremental formulation is derived here. A coordinate system is oriented with the X-direction parallel to the weld direction, and the Y-direction parallel with the in-plane perpendicular direction. The Z-direction is parallel to the out of plane normal (see Figure 5). The user subroutine is formulated around using the middle of the plate thickness as the reference Z-position.

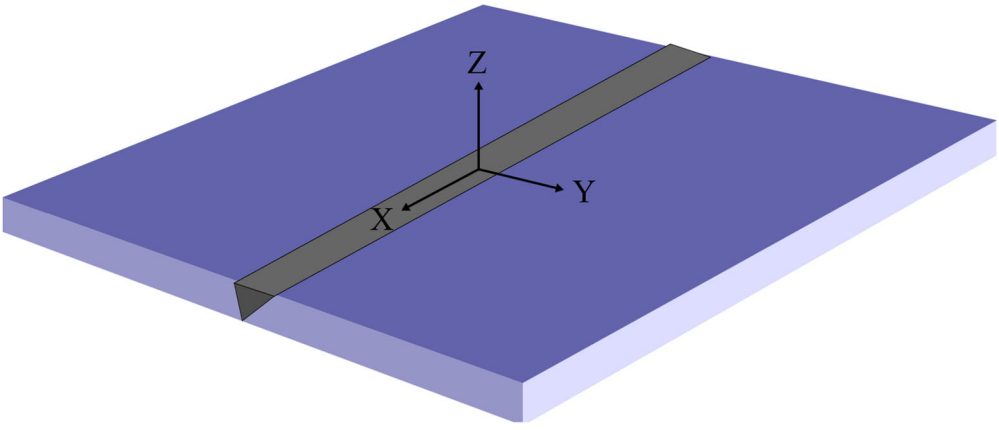


Figure 5. Plate coordinate system.

A scaling parameter was employed to ensure stability of complex structures. This scaling parameter, φ, linearly varies with respect to time between the initial activation time, t_a, and the fully activated time, t_s so that $\varphi = 0$ at t_a and $\varphi = 1$ at t_s. UEXPAN does not provide any direct information on the position of the section point, and it requires the derivative of the thermal strains with respect to the temperature to construct the tangent for Newton–Raphson iterations. The former can be circumvented by applying a unit temperature gradient to the shell element, which in turn turns the section point temperature equal to the section point Z-position. Regarding the latter, a uniform temperature equal to

the φ is assigned to the midsection, T_m, such that $T_m = 0$ at t_a and $T_m = 1$ at t_s. Figure 6 depicts the applied temperature field for a given element.

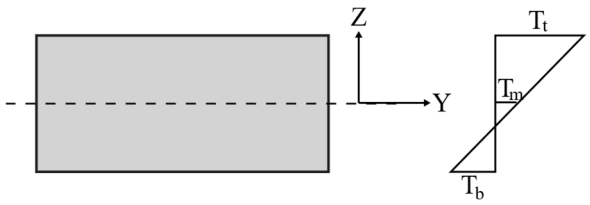


Figure 6. Plate neutral axis and the applied temperature gradient.

The applied uniform temperature offsets the temperature gradient, and the position of the section point may then be found by:

$$z = \frac{T_s - \varphi}{\varphi} \tag{1}$$

Here, z is the section point Z-coordinate and T_s is the temperature of the section point. The total applied inherent strain of the section point in the x-direction, ε_x, can be found using:

$$\varepsilon_x = \varepsilon_{x,u} + z \cdot \kappa_x \tag{2}$$

Here, $\varepsilon_{x,u}$ is the uniform strain component in the x-direction, and κ_x is the curvature in the x-direction. The total applied inherent strain of the section point in the y-direction, ε_y, is found using a similar expression, however the components are replaced with the respective y-direction counterparts:

$$\varepsilon_y = \varepsilon_{y,u} + z \cdot \kappa_y \tag{3}$$

The increment in the scaling factor is $\Delta\varphi_{n+1} = \varphi_{n+1} - \varphi_n$, and its computation is constrained to ensure that the sum of all the increments in scaling factors between t_a and t_s remain 1, further that the sum remains 1 for $t \to \infty$.

$$\Delta\varepsilon_{x,n+1} = \Delta\varphi_{n+1}\varepsilon_x \tag{4}$$

$$\Delta\varepsilon_{y,n+1} = \Delta\varphi_{n+1}\varepsilon_y \tag{5}$$

Lastly, the derivative of the strain components with respect to temperature, is found by applying a numerical perturbation scheme.

2.2.3. 3D Shell "Low-Fidelity" Model

The low-fidelity model was established using 10 mm × 10 mm S4R elements, except for the outer row that was 10 mm × 15 mm S4R elements (see Figure 7). A local material coordinate system is applied to the model to ensure that the inherent strain is correctly applied, and the shell element normal is set parallel to the material Z-direction. The latter part is conducted to ensure that the applied temperature gradient shown in Figure 6 correctly describes the Z-position. The elements are given an elastic modulus of 70,000 MPa and a Poisson's ratio of 0.3. The inherent strain field applied to the model is applied to each row spanning out from the welded joint. Only two of four inherent deformations were applied to the model, namely the transverse shrinkage and transverse bending. Longitudinal shrinkage and longitudinal bending were not considered in this work.

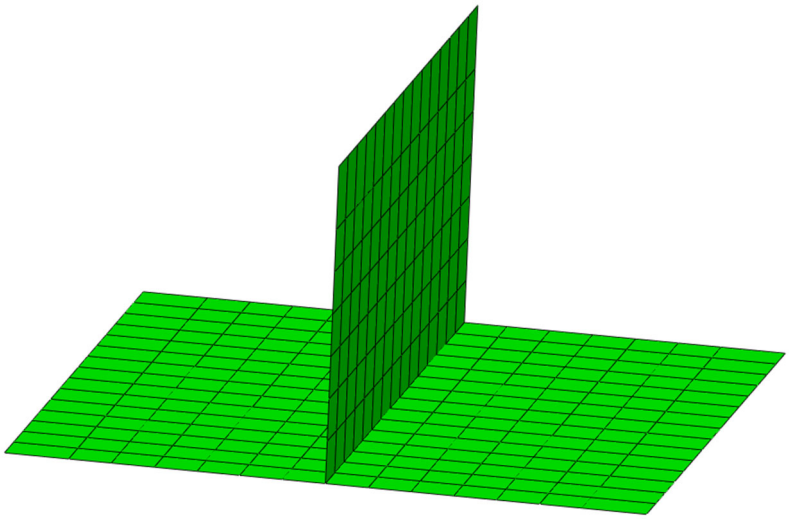


Figure 7. The shell element mesh of the "low-fidelity" model.

3. Results

The welded specimens were quite consistent. One of the specimens was selected for measuring the out of plane distortions of P2. The experimental results are shown in Figure 8. A local coordinate system was applied to one of the corners of P2, and the measurements were expressed in the local coordinate system to quantify the distortions. This coordinate system corresponds to the coordinate system of Figure 5 with the origo placed in the bottom left corner. The Z-axis are purposely not in scale to emphasize the out of plane distortion. The relative distortions are significant with a maximum value approaching 5 mm. Both transverse bending and longitudinal bending are visible in the results.

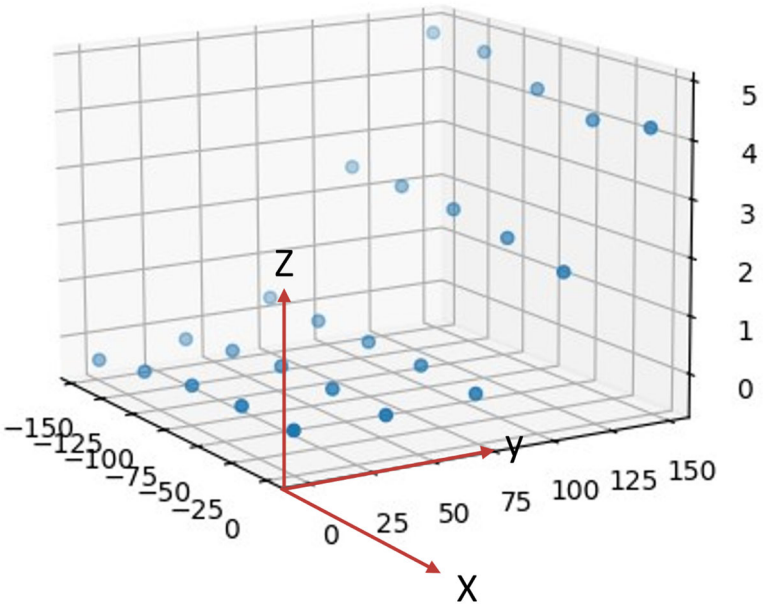


Figure 8. Out of plane distortions of the P2 plate.

The results of the "high-fidelity" thermo-mechanical model is shown in Figure 9. The out of plane distortion reaches a magnitude of 3 mm to 4 mm on the right edge of P2. Both longitudinal and transverse bending are visible in the figure.

https://doi.org/10.3390/engproc2026151032

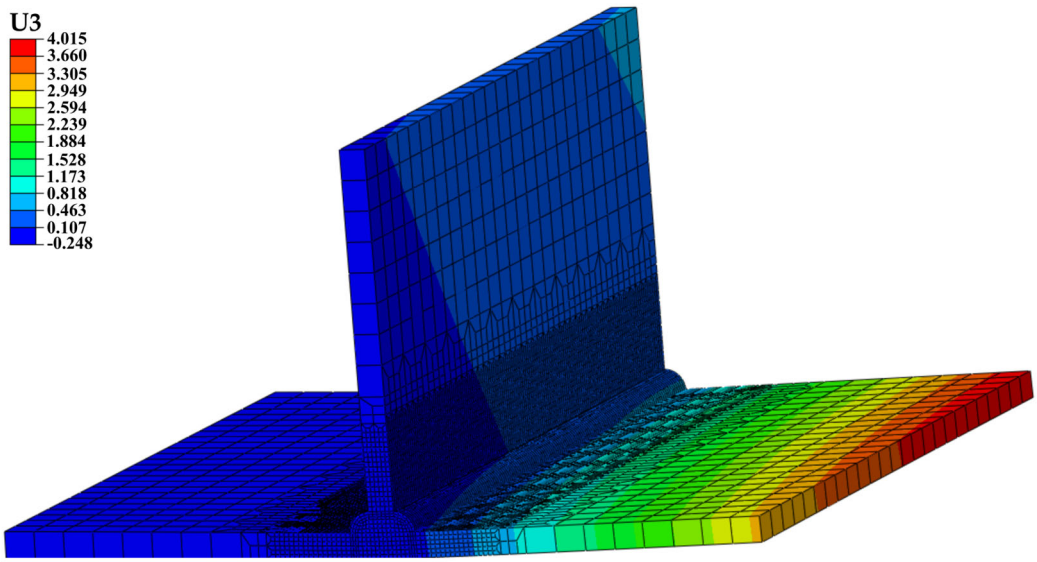


Figure 9. Numerical results from the "high-fidelity" model depicting displacements in the Z-direction.

The results from the "low-fidelity" model are shown in Figure 10. Here, it is seen that the model does not describe any longitudinal bending, and a maximum deflection of 4.2 mm is estimated.

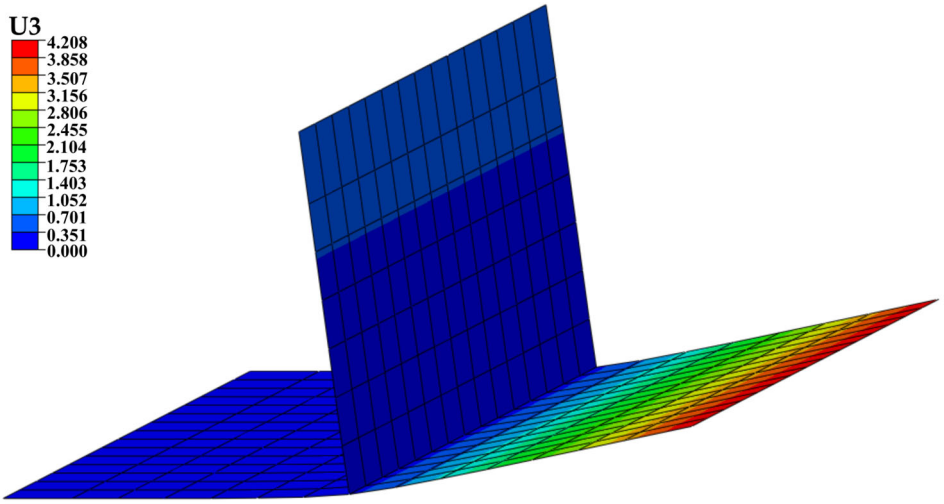


Figure 10. Numerical results from the "low-fidelity" model depicting displacements in the Z-direction.

4. Discussion

The "high-fidelity" model is clearly not optimized. The out of plane distortion is underestimated by about 20%. However, the model can reproduce the visible trend, i.e., longitudinal bending in addition to transverse bending. The lack of differentiation between the 5183 welding wire and 6082 plate material and using "generalized" parameters for aluminum are substantial sources of errors. The lack of optimization is strictly due to the down priority of the model, as the development, implementation and debugging of the "low-fidelity" model has been the focus of the current work. When comparing the "high-fidelity" and "low-fidelity" models it is apparent that the "low-fidelity" models over-estimate the out of plane distortions based upon the results from the "high-fidelity" model. To investigate this, a simplified benchmarking model was established. The model consisted of five shell elements (1 × 1 size), and element 1 (from the left) was given a negative curvature of 0.05, and the fourth element was given a positive curvature of 0.05.

The analytical solution to this problem is an upward deflection of 0.15 mm, and a zero angle of the fifth element. The deflection is clearly captured by the elements as seen in Figure 11, as well as the zero angle for the fifth element.

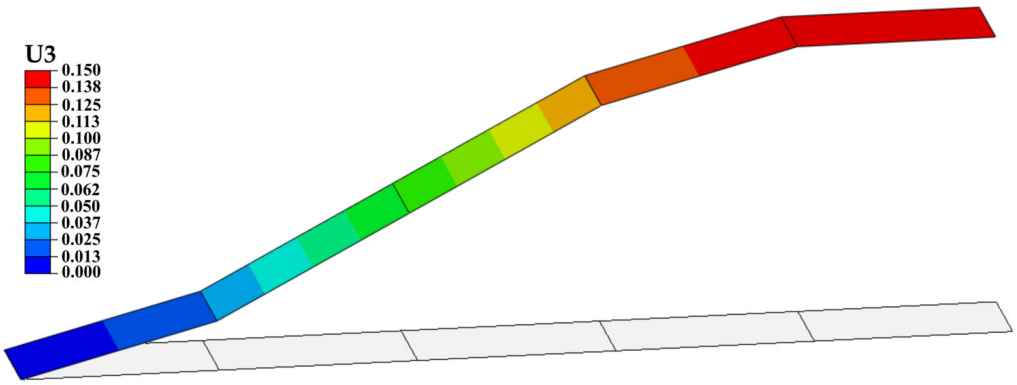


Figure 11. Simplified benchmark model.

This indicates that the post-processing procedure might have introduced errors into the applied inherent strains. Further, mathematically, the direct description of inherent strains is capable of reproducing the exact same deformation modes as the layered approach, meaning that for a given inherent strain field the resulting deformation field will be equal using either method. In addition, current frameworks utilizing the layered approach may be adapted to use the direct description with little effort.

5. Conclusions

A new method of introducing inherent strains into 3D shell element models was proposed. The method is mathematically capable of describing the same deformation modes as the layered approach and may therefore be easily implemented into current modelling frameworks. There was a discrepancy between the experimental and numerical results, and the non-optimized 3D solid thermo-mechanical model which is used as a source for the inherent strain is a major contributor to the accumulated error. Further, the omission of longitudinal bending, and the post-processing procedure contributed to the discrepancy between the two numerical models. It is evident that future work is required on optimizing the source of inherent strains, i.e., the 3D solid thermo-mechanical model, and that a more robust post-processing script is required.

Author Contributions: Conceptualization, A.J.T., I.B. and M.E.; methodology, A.J.T.; software, A.J.T. and I.B.; investigation, I.B.; formal analysis, A.J.T.; data curation, A.J.T. and I.B.; writing—original draft preparation, A.J.T.; writing—review and editing, A.J.T., I.B. and M.E.; supervision, M.E.; project administration, A.J.T., I.B. and M.E.; funding acquisition, A.J.T. and M.E. All authors have read and agreed to the published version of the manuscript.

Funding: This research was fully funded by an internal proof of concept programme at SINTEF Industry, and the research has therefore not received any external funding.

Institutional Review Board Statement: Not applicable.

Informed Consent Statement: Not applicable.

Data Availability Statement: The experimental data and the 3D solid thermo-mechanical framework are not publicly available due to ongoing research. The direct description subroutine can be shared upon request.

Acknowledgments: The authors would like to thank SINTEF Industry for providing financial support for the proof of concept.

Conflicts of Interest: The authors declare no conflicts of interest.

References

1. Ueda, Y.; Fukuda, K. New Measuring Method of Three-Dimensional Residual Stresses in Long Welded Joints Using Inherent Strains as Parameters—L_z Method. *J. Eng. Mater. Technol.* **1989**, *111*, 1–8. [CrossRef]
2. Murakawa, H.; Deng, D.; Ma, N. Concept of inherent strain, inherent stress, inherent deformation and inherent force for prediction of welding distortion and residual stress. *Trans. JWRI* **2010**, *39*, 103–105. [CrossRef] [PubMed]
3. Deng, D.; Murakawa, H.; Liang, W. Numerical simulation of welding distortion in large structures. *Comput. Methods Appl. Mech. Eng.* **2007**, *196*, 4613–4627. [CrossRef]
4. Deng, D.; Murakawa, H. FEM prediction of buckling distortion induced by welding in thin plate panel structures. *Comput. Mater. Sci.* **2008**, *43*, 591–607. [CrossRef]
5. Deng, D.; Murakawa, H.; Ma, N.; Serizawa, H. Application of inherent deformation and interface element to prediction of welding distortion during assembly process. *Trans. JWRI* **2010**, *39*, 109–111. [CrossRef] [PubMed]
6. Yang, Y.P.; Jung, G. Advancement in Prediction and Control of Welding Residual Stress and Distortion. *Mater. Sci. Forum* **2007**, *539–543*, 3943–3948. [CrossRef]
7. Jung, G. Plasticity-Based Distortion Analysis for Fillet Welded Thin Plate T-Joints. Doctoral Dissertation, The Ohio State University, Columbus, OH, USA, 2003.
8. Liang, W.; Hu, X.; Zheng, Y.; Deng, D. Determining inherent deformations of HSLA steel T-joint under structural constraint by means of thermal elastic plastic FEM. *Thin-Walled Struct.* **2020**, *147*, 106568. [CrossRef]
9. Mao, Z.; Liang, W.; Yuan, F.; Deng, D. Predicting Welding Deformation of Mild Steel Bead-on-Plate Joints by Means of Artificial Neural Network and Inherent Strain Method. *J. Manuf. Processes* **2025**, *142*, 424–439. [CrossRef]
10. Totonchi, B.A.; Aghazadeh, K.; Zakeri, B.; Attarnejad, R. Distortion analysis and optimization of grillage structure assembly process by finite element inherent strain method (FE-ISM)-part 1: Connector element as a new weld interface model. *Weld. World* **2026**, *70*, 3711–3732. [CrossRef]
11. Han, Y.-H.; Noh, H.-J.; Yoon, H.-C.; Lim, H.-B.; Yang, H.-I. Predicting multi-pass welding distortion using the strain as directed boundary method considering interpass. *J. Mech. Sci. Technol.* **2023**, *37*, 4039–4045. [CrossRef]
12. Bunaziv, I.; Akselsen, O.M.; Frostevarg, J.; Kaplan, A.F.H. Laser-arc hybrid welding of thick HSLA steel. *J. Mater. Process. Technol.* **2018**, *259*, 75–87. [CrossRef]

Disclaimer/Publisher's Note: The statements, opinions and data contained in all publications are solely those of the individual author(s) and contributor(s) and not of MDPI and/or the editor(s). MDPI and/or the editor(s) disclaim responsibility for any injury to people or property resulting from any ideas, methods, instructions or products referred to in the content.